BNL-108192-2015-JA

Direct Observation of Xe and Kr Adsorption in a Xe-selective Microporous Metal Organic Framework

Xianyin Chen[1], Anna M. Plonka[2], Debasis Banerjee[3], Rajamani Krishna[4], Herbert T. Schaef[3], Sanjit Ghose[5], Praveen K. Thallapally[3,*] and John B. Parise[1,2,5,*]

[1]Department of Chemistry, Stony Brook University, Stony Brook, NY 11794, USA

[2]Department of Geosciences, Stony Brook University, Stony Brook, NY 11794, USA

[3]Fundamental & Computational Science Directorate, Pacific Northwest National Laboratory, Richland, WA 99352, USA

[4]Van't Hoff Institute for Molecular Sciences, University of Amsterdam, Science Park 904, 1098 XH Amsterdam, The Netherlands

[5]Photon Sciences, Brookhaven National Laboratory, Upton, NY 11973, USA

Supporting Information

ABSTRACT: The cryogenic separation of noble gases is energy-intensive and expensive, especially when low concentrations are involved. Metal organic frameworks containing polarizing groups within their pore spaces are predicted to be efficient Xe/Kr solid state adsorbents but no experimental insights into the nature of the Xe-network interaction are available to date. Here we report a new microporous metal organic framework (designated SBMOF-2) that is selective toward Xe over Kr at ambient conditions, with Xe/Kr selectivity of about 10 and Xe capacity of 27.07 wt% at 298 K. Results of single crystal diffraction show the Xe selectivity may be attributed to the specific geometry of the pores, forming cages built with phenyl rings and enriched with polar -OH groups, both serving as strong adsorption sites for polarizable Xe gas. The Xe/Kr separation in SBMOF-2 was investigated with experimental and computational breakthrough methods. These experiments showed that Kr broke through the column first followed by Xe, which confirmed that SBMOF-2 has a real practical potential for separating Xe from Kr. Computational calculations show that SBMOF-2 capacity and adsorption selectivity is comparable to the best-performing unmodified MOFs such as NiMOF-74 or Co Formate.

The increasing global energy demand drives the search for alternative, low-polluting sources of energy, as fossil-fuel combustion is non-sustainable from both economic and environmental perspectives. Currently, nuclear fission, with the highest energy density when compared to other power sources[1], is the leading, emission-free technology, for supply of base load power. Apart from preventing fossil fuel related carbon emission, it is estimated that utilization of nuclear power has prevented an average of 1.84 million air pollution-related deaths.[2] Further development of nuclear fuel as a major energy source requires implementation of efficient and economically viable industrial-scale processes that separate and sequester highly radioactive waste during fuel rod reprocessing.[3] Reprocessing minimizes the volume of high-level radioactive waste, and amongst the most important steps in reprocessing is mitigating the volume of radioactive waste. The economical separation of Xe/Kr from each other is important to sequester and mitigate the radioactive Kr in nuclear reprocessing technology. As radioactive ^{127}Xe has a half-life of 36.3 days, short-time storage of radioactive Kr/Xe mixtures and later separation of ^{85}Kr ($t_{1/2}$ = 10.8 years) from stable Xe will significantly reduce the volume of long-term stored radioactive waste and provide industrially useful Xe. Efficient separation at near room temperature at very low pressure would ultimately compete with cryogenic technology currently used in nuclear reprocessing and air separation.

Xe/Kr separation using selective solid state adsorbent is a viable alternative to cryogenic distillation and many porous materials such as organic cages, and modified zeolites such as Ag-natrolite, were extensively tested by experimental and computational methods.[4a-c] For example, Cooper and coworkers reported Xe-selective porous organic cages, where selectivity arises from precise size match between the rare gas and the organic cage cavity.[4a]

Metal organic frameworks (MOFs) are a relatively new class of materials, based on metal ions and organic ligands forming microporous frameworks. The variety of compositions capable of forming MOFs, along with their modification post-synthesis, facilitates the tailoring of pore geometry and chemistry for specific applications.[5] Only a handful of noble gas adsorption studies in MOFs are presented in literature.[6a-k] Thallapally et al. noted a

15% enhancement in the Xe adsorption capacity in Ni-MOF-74 after depositing Ag nanoparticles.[7] These authors also observed a higher Xe/Kr selectivity and rationalized their results by invoking stronger interactions between polarizable Xe molecules and the well-dispersed Ag nanoparticles.

So far, only a handful of MOFs have been tested for Xe/Kr separation and given the large number of suitable MOFs present in the literature, there is certainly scope for improvement through discovery of more selective materials than the materials studied to date.[8a-c] Because Xe/Kr separation is based on the small difference in size and polarizability, it is expected that narrow pores, and pores enriched with polar groups or unsaturated metal centers, will increase Xe-affinity, resulting in better separation of Xe from Kr.[1, 9] Despite this conclusion there are no experimental reports of the molecular level interactions between gas and framework, and this limits the reliability of theoretical calculations that could rapidly screen for selectivity and capacity. To better understand optimal framework characteristics it is essential to directly study the adsorption mechanism, and experimental structural analysis provides the most detailed picture of adsorbate-adsorbent interactions.

Here we report the synthesis and Xe/Kr sorption properties of a robust 3-D porous crystalline structure containing calcium and 1,2,4,5-tetrakis(4-carboxyphenyl)benzene, a new MOF named SBMOF-2:H2O (Stony Brook MOF-2). The dehydrated form, designated SBMOF-2, adsorbs Xe at a capacity of 27.07 wt% at 298 K and with high Xe/Kr selectivity of approximately 10 at 298K; these results are extraordinary for an unmodified MOF. We examined the Xe and Kr adsorption mechanism by interpreting the results of single crystal X-ray diffraction (XRD), and observed significant differences for Xe versus Kr, noting differentiation between polar and non-polar pores in SBMOF-2. Although polar pores occur in other MOFs,[9] the differentiation of sorbed gases between them, as occurs in SBMOF-2, is not reported for MOFs.

The structure of SBMOF-2:H2O is unusual amongst microporous MOFs.[10] Only half of the carboxylic groups are fully deprotonated and the network contains half of the expected Ca^{2+} sites (Figure S1). Charge balance provided by hydrogen, not heavier calcium, leads to the low density of the dehydrated material (1.192 g/cm^3) which is comparable to MOFs with significantly higher surface areas, such as HKUST-1 (0.879 g/cm^3) and MgMOF-74 (0.909 g/cm^3).[11] The half-deprotonated linker connects the calcium octahedra into a 3-D framework with diamond-shaped channels running in [100] (Figure S2-S3). The excess of oxygen versus calcium also leads to a topology that is unusual for MOF synthesized from s-block metals; CaO_6 polyhedra are isolated and no O atoms are shared between metal centers. To the best of our knowledge, SBMOF-2 is the first microporous 3-D MOF network with isolated CaO_6 octahedra connected by linkers.

Thermo-gravimetric Analysis (TGA; Figure S4) indicates that as-synthesized SBMOF-2:H2O contains 6.5 wt% of water, which can be removed by heating to 513 K in vacuum. Single crystal and powder XRD experiments (Figure S5, Table S1) show that water is disordered over sites within channels, and that after dehydration SBMOF-2 retains its structure, with a small change in the unit cell volume of ~3%. The accessible void space equals 25.6% of the unit cell (212.5 Å^3 out of 831.4 Å^3, calculated with PLATON[12]). The two different types of channels designated as type-I and type-II in Figure 1 have walls built with phenyl rings with delocalized π-electron clouds and H-atoms pointing into the channel, providing potential sorption sites for gas molecules. The polar -OH groups are found exclusively in channels of type-II and serve as more polarizing parts in the network, resulting in significantly higher occupancy of the adsorbed noble gases. The void space of channels type-I and type-II is 13.6% and 12% of the unit cell, respectively. BET measurements showed that SBMOF-2 has a moderate surface area of 195 m^2/g; the N2 adsorption isotherm at 77 K is shown in Figure S6.

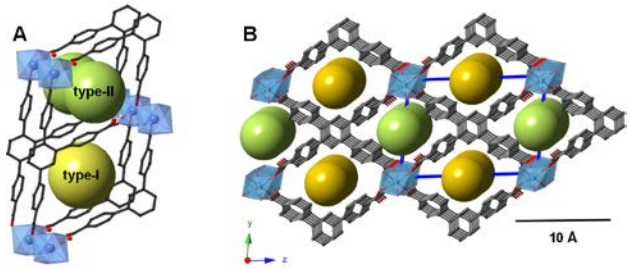

Figure 1. (A) Structure of the activated SBMOF-2. The colored spheres indicate estimated channel apertures, for channel type-I: 6.34 Å for channel type-II: 6.66 Å, color coded: yellow – type-I, green – type-II. (B) Pores running along [100]. The octahedral coordination around calcium is presented as blue polyhedra, oxygen – red spheres and carbon – grey wire bonds. Hydrogen atoms are omitted for clarity. Unit cell is shown in blue.

Activated SBMOF-2 maintains its topology when exposed to air for 5 days, as observed from TGA and powder XRD patterns. Additionally TGA measurements show that SBMOF-2 does not saturate with water from air for 5 days. (Figure S7-S8)

The stability in air, small pore/channel size closer to the size of atomic xenon, and the lightweight character of the SBMOF-2 suggested it might possess good gas sorption and separation properties, and indeed this material is remarkable at separating Xe from Kr. Adsorption/desorption of Xe and Kr on SBMOF-2 at 278, 288 and 298 K are shown in Figure 2A. Both gases display a typical type-I adsorption isotherm but Xe uptake is more than 3 times higher - 2.83 mol/kg (27.07 wt %) versus 0.92 mol/kg (7.18 wt %) for Kr at 298 K. Although the uptake of Xe in SBMOF-2 is lower than the observed for well-known rare noble gas adsorbents with open metal sites, such as NiMOF-74 and Ag@Ni-MOF74 where the sorption capacity is 3.6 mol/kg and 4.8 mol/kg, respectively,[6d, 7] structures with open metal sites usually suffer from water sensitivity. The uptake is higher than in Co Formate (2 mol/kg) and organic cages (2.69 mol/kg) which do not have open metal sites.[4a, 8b] The Xe isotherm approaches

saturation at 1 bar with the gas occupancy of 1.68 molecules per unit cell at 298 K, which corresponds to a maximum of 2 gas molecule per unit cell, suggesting that Xe is ordered on specific sorption sites.

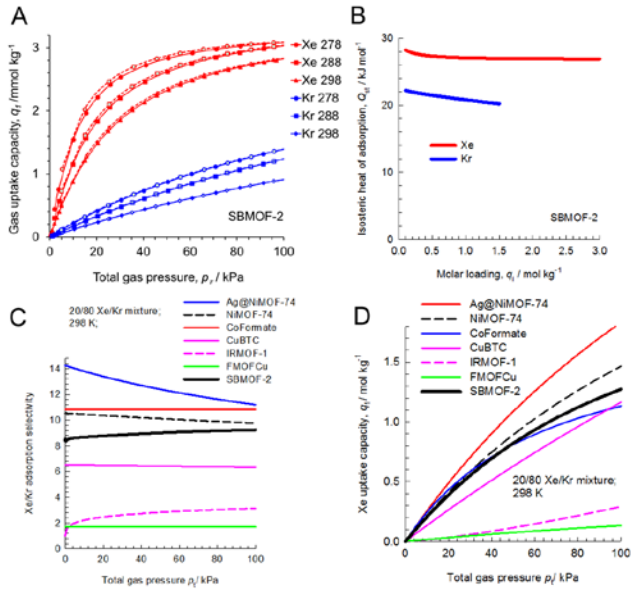

Figure 2. Kr/Xe adsorption and selectivity in SBMOF-2 (A) Single component adsorption isotherms (solid symbols) and desorption isotherms (open symbols) of Xe (red) and Kr (blue) in SBMOF-2 collected at 278, 288 and 298 K. (B) Isosteric heat of adsorption for Xe/Kr@SBMOF-2. Calculated (C) adsorption selectivities, and (D) Xe uptake capacities for 20/80 Xe/Kr mixtures in SBMOF-2 and comparison with other compounds.[1]

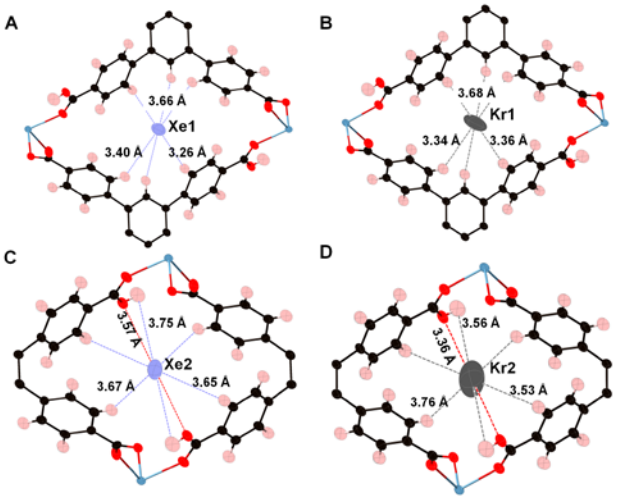

Figure 3. (A, C) Xe sorption sites determined from single crystal XRD experiments. (B, D) Kr sorption sites determined from single crystal XRD experiments. Site positions of Xe and Kr in the two channels are similar, with both located at (0.5, 0, 0.5) and (0.5, 0.5, 0).

The heat of interaction (Qst) between adsorbed noble gases and the SBMOF-2 network was determined by analysis of the gas isotherms. Both Xe and Kr isotherm data at 278 K, 288 K and 298 K were fitted with the dual-Langmuir-Freundlich model (Figure S9, Table S2) and the Qst was calculated using the Clausius-Clapeyron equation. As expected, the values for Xe adsorption are higher than that of Kr, indicating stronger biding (26.4 vs. 21.6 kJ/mole). (Figure 2B).

Single crystal diffraction results indicate Xe ordering with two distinct adsorption sites in channels of type-I and type-II. The absorption of 1.45 molecule per unit cell, determined from diffraction, agrees with the 1.68 molecule per unit cell determined from isotherm measurements.(Figure 2A) The lower interaction potential for Kr, resulting from its smaller size and polarizabilty, explains the lower Kr occupancy (0.51 vs. 0.66 from isotherm) at one atmosphere. In both structures of SBMOF-2:Xe and SBMOF-2:Kr, occupancy of gas atoms in channel of type-I is lower than in type-II because of the more polarizing -OH groups present in the latter.

In channel type-I, Xe is surrounded by H atoms from phenyl rings with the shortest Xe...H distance of 3.268(9) Å. While in channel type-II the shortest Xe...H distance is 3.646(6) Å and Xe...O distance is 3.567(5) Å (Figure 3 A-D). The average Xe...H distance of 3.568(8) Å in the channels of SBMOF-2:Xe is slightly shorter than the average Xe...H contact distance in literature 3.71(4) Å,[4a] suggesting that small pore aperture is increasing the energy of network-gas interaction by surrounding Xe with many H atoms in close proximity. Kr occupies two similar sorption sites as those found for SBMOF-2:Xe, with the shortest Kr...H distance in channel type-I of 3.342(3) Å, and 3.545(3) Å plus a Kr...O 3.364(4) Å in type-II. The observed longer distances between H and Kr in comparison to H and Xe atoms is consistent with the Xe selectivity in SBMOF-2 being driven by larger size and stronger polarizability of Xe atoms compared to Kr. The observed Xe...Xe contact distance of 5.1812(3) Å is longer than in both crystalline Xe (4.3 Å) and in high pressure induced Xe dimers.[13a-c] Similar adsorption sites are observed in Kr-loaded structure with a Kr...Kr distance of 5.11(1) Å.

The SBMOF-2 Xe/Kr selectivity and Xe capacity for the 20/80 mixtures at 298 K was calculated with ideal adsorbed solution theory (IAST) of Mayers and Prausnitz using fitted isotherms.[14] The results are presented in Figure 2C-D. For comparison purposes, the corresponding data for NiMOF-74, Ag@NiMOF-74, CuBTC, IRMOF-1, FMOF-Cu, and Co Formate are also included. At 100 kPa, SBMOF-2 shows the Xe/Kr adsorption selectivity of about 10, comparable to the value for NiMOF-74.[6a, 7]

Simulation breakthrough is commonly calculated to estimate the separation of Xe/Kr mixtures. For a 20/80 Xe/Kr feed mixture at 100 kPa and 298 K, Figure S10 A shows the reduced concentrations at the outlet of a fixed bed adsorber as a function of the dimensionless time, $\tau = tu/L\varepsilon$. On the basis of the outlet gas compositions, we can determine the ppm Xe in the outlet gas as a function of τ; see Figure S10 B. The corresponding data for NiMOF-74, Ag@NiMOF-74, CuBTC, IRMOF-1, FMOF-Cu, and Co Formate are also included for comparison purposes. On the basis of Figure S10 B, the breakthrough time for SBMOF-2 is slightly lower than that of NiMOF-74 and Ag@NiMOF-74.

To supplement the simulated breakthrough, experimental breakthrough experiments were carried out to further demonstrate the Xe/Kr separation ability in both 1/1 Kr/Xe concentration and low gas concentration, in conditions expected for spent nuclear fuel reprocessing. 130 mg of SBMOF-2 was packed in a column and the sample was activated at 513 K in flowing He overnight. After cooling to room temperature, mixtures of gases (5% Kr, 5% Xe and 90% N_2 by volume) were introduced to the column. After injection of the gas mixture, Kr broke through the column after ~20 min followed by Xe after ~40min, suggesting preferable adsorption and selectivity towards Xe over Kr by SBMOF-2 (Figure 4). The adsorption capacity of Xe (0.80 mol/kg) under column breakthrough experiments is matched with Xe adsorption via static method (0.85 mol/kg) at 0.07 bar. The experimental breakthrough measurements confirm that the adsorption kinetics in SBMOF-2 is fast enough for separation of Xe over Kr.

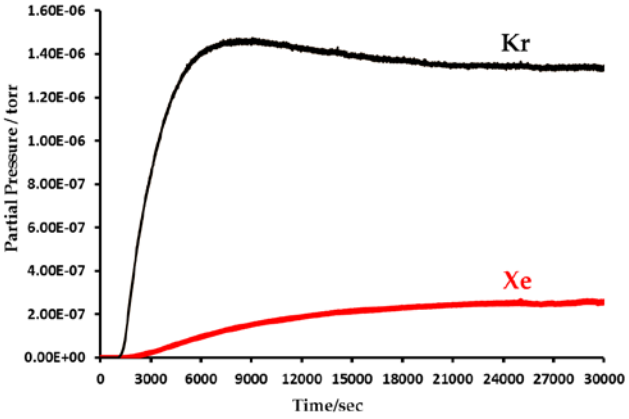

Figure 4. Breakthrough experiments show separation of Xe and Kr at 5% Kr and 5% Xe.

In summary, the new 3-D porous material SBMOF-2 has an unprecedented structure with two different hydrogen rich channels; Xe is strongly adsorbed in pores enriched with more polarizing –OH groups. The geometry of the channels, best matched for the larger Xe atoms rather than smaller Kr, also helps explain the selectivity of Xe over Kr.

ASSOCIATED CONTENT

Supporting Information

Crystallographic data are available free of charge from Cambridge Crystallographic Data Center under reference numbers (CCDC 1039468-1039471). Experimental details, additional figures as mentioned in the text, and simulations are provided. This material is available free of charge via the Internet at http://pubs.acs.org.

AUTHOR INFORMATION

Corresponding Author

john.parise@stonybrook.edu
praveen.thallapally@pnnl.gov

Notes

The authors declare no competing financial interests.

ACKNOWLEDGMENT

This work is supported by the U.S. DOE Office of Sciences, Office of Basic Energy Science (DE-FG02-09ER46650), DOE Office of Nuclear Energy, DOE by Battelle Memorial Institute (DE-AC05-76RL01830) and NSF (CHE-0840483). We would like to acknowledge in particular: J. Bresee, T. Todd (Idaho National Laboratory) and B. Jubin (Oak Ridge National Laboratory), who provided programmatic support and guidance.

REFERENCES

(1) Banerjee, D.; Cairns, A. J.; Liu, J.; Motkuri, R. K.; Nune, S. K.; Fernandez, C. A.; Krishna, R.; Strachan, D. M.; Thallapally, P. K. *Acc. Chem. Res.* **2015**, 48(2), 211.
(2) Kharecha, P. A.; Hansen, J. E. Environmental *Envir. Sci. & Tech.* **2013**, 47, 4889.
(3) Soelberg, N. R.; Garn, T. G.; Greenhalgh, M. R.; Law, J. D.; Jubin, R.; Strachan, D. M.; Thallapally, P. K. *Sci. Tech. Nucl. Inst.* **2013**, 2013, 1.
(4) (a) Chen, L.; Reiss, P. S.; Chong, S. Y.; Holden, D.; Jelfs, K. E.; Hasell, T.; Little, M. A.; Kewley, A.; Briggs, M. E.; Stephenson, A.; Thomas, K. M.; Armstrong, J. A.; Bell, J.; Busto, J.; Noel, R.; Liu, J.; Strachan, D. M.; Thallapally, P. K.; Cooper, A. I. *Nat. Mat.* **2014**, 6, 835. (b) Seoung, D.; Lee, Y.; Cynn, H.; Park, C.; Choi, K. Y.; Blom, D. A.; Evans, W. J.; Kao, C. C.; Vogt, T.; Lee, Y. *Nat Chem* **2014**, 6, 835. (c) Bazan, R. E.; Bastos-Neto, M.; Moeller, A.; Dreisbach, F.; Staudt, R. *Adsorption* **2011**, 17, 371.
(5) Stock, N.; Biswas, S. *Chem. Rev.* **2012**, 112 (2), 933.
(6) (a) Liu, J.; Thallapally, P. K.; Strachan, D. *Langmuir* **2012**, 28, 11584. (b) Wang, H.; Yao, K.; Zhang, Z.; Jagiello, J.; Gong, Q.; Han, Y.; Li, *J. Chem. Sci.* **2014**, 5, 620. (c) Lawler, K. V.; Hulvey, Z.; Forster, P. M. *Chem. Commun.* **2013**, 49, 10959. (d) Thallapally, P. K.; Grate, J. W.; Motkuri, R. K. *Chem. Commun.* **2012**, 48, 347. (e) Sikora, B. J.; Wilmer, C. E.; Greenfield, M. L.; Snurr, R. Q. *Chem Sci* **2012**, 3, 2217. (f) Ueda, T.; Kurokawa, K.; Eguehit, T.; Kachi-Terajima, C.; Takamizawa, S. *J. Phys. Chem. C* **2007**, 111, 1524. (g) Dorcheh, A. S.; Denysenko, D.; Volkmer, D.; Donner, D.; Hirscher, M. *Micropor. Mesopor. Mater.* **2012**, 162, 64. (h) Bae, Y.; Hauser, B. G.; Colón, Y. J.; Hupp, J. T.; Farha, O. K.; Snurr, R. Q. *Micropor. Mesopor. Mater.* **2013**, 169, 176. (i) Fernandez, C. A.; Liu, J.; Thallapally, P. K.; Strachan, D. M. *J. Am. Chem. Soc.* **2012**, 134, 9046. (j) Heest, T. V.; Teich-McGoldrick, S. L.; Greathouse, J. A.; Allendorf, M. D.; Sholl, D. S. *J. Phys. Chem. C* **2012**, 116, 13183. (k) Perry, J. J.; Teich-McGoldrick, S. L.; Meek, S. T.; Greathouse, J. A.; Haranczyk, M.; Allendorf, M. D. *J. Phys. Chem. C* **2014**, 118, 11685.
(7) Liu, J.; Strachan, D. M.; Thallapally, P. K. *Chem. Commun.* **2014**, 50, 466.
(8) (a) DeCoste, J. B.; Peterson, G. W. *Chem. Rev.* **2014**, 114, 5695. (b) James, S. L. *Chem. Soc. Rev.* **2003**, 32, 276. (c) Chae, H. K.; Siberio-Pe´rez, D. Y.; Kim, J. C.; Go, Y.; Eddaoudi1, M.; Matzger, A. J.; O'Keeffe, M.; Yaghi, O. M. *Nature* **2004**, 427, 522.
(9) Magdysyuk, O. V.; Adams, F.; Liermann, H. P.; Spanopoulos, I.; Trikalitis, P. N.; Hirscher, M.; Morris, R. E.; Duncan, M. J.; McCormick, L. J.; Dinnebier, R. E. *Phys. Chem. Chem. Phys.* **2014**, 16, 23908.
(10) Zhu, Q. L.; Xu, Q. *Chem. Soc. Rev.* **2014**, 43, 5468.
(11) He, Y.; Zhou, W.; Krishna, R.; Chen, B. *Chem. Commun.* **2012**, 48, 11813.
(12) Spek, A.L. Acta Cryst. **2009**, D65, 148.
(13) (a) Somayazulu, M.; Dera, P.; Goncharov, A. F.; Gramsch, S. A.; Liermann, P.; Yang, W.; Liu, Z.; Mao, H. K.; Hemley, R. *J. Nature Chem.* **2010**, 2, 50. (b) Natta, G.; Nasini, A. G. *Nature* **1930**, 125, 457. (c) Sears, D. R.; Klug, H. P. *J Chem. Phys.* **1962**, 37, 3002.
(14) Myers, A. L.; Prausnitz, J. M. *A.I.Ch.E.J.* **1965**, 11, 121.

Table of Contents Graphic